The hyporeflective fern-like pattern on deep-layer en face images of acute central retinal artery occlusion

Junki Hoshino
Gunma university graduate school of medicine
Hideo Akiyama (akiyamah47@gunma-u.ac.jp)
Gunma university graduate school of medicine
Mikiya Magori
Gunma university graduate school of medicine
Ryo Mukai
Gunma university graduate school of medicine
Hidetaka Matsumoto
Gunma university graduate school of medicine

Research article

Keywords: Central retinal artery occlusion; Fern like pattern; En face image

Posted Date: August 12th, 2019

DOI: https://doi.org/10.21203/rs.2.12603/v1

Abstract

Background We examined B-mode and en face images of swept-source optical coherence tomography (SS-OCT) from patients with central retinal artery occlusion (CRAO), and investigated associations between their characteristics and prognosis for visual acuity. Methods We retrospectively investigated 11 eyes in 11 patients with CRAO who underwent swept-source OCTA (PLEX Elite 9000®; Carl Zeiss, Dublin, California, USA) and SS-OCT (DRI OCT-1 Atlantis, Topcon, Tokyo, Japan) at the acute phase and 1 month after onset. Results Fern-like hyporeflective patterns aligned with the superficial arterioles were observed in acute-phase deep-layer en face images from 4 patients. Patients who exhibited these hyporeflective fern-like patterns were categorized as Group A, and all other patients as Group B. No significant difference in best-corrected visual acuity at initial examination was seen between the groups. At one month after onset, best-corrected visual acuity was significantly better in Group A, and retinal thinning also tended to be milder. Conclusions Our results indicate that a hyporeflective fern-like pattern in acute CRAO may suggest good prognosis.

Background

Central retinal artery occlusion (CRAO) is a retinal vascular disorder in which sudden severe loss of vision occurs as a result of embolic or thrombotic occlusion of the central retinal artery. The diagnosis is usually made based on the medical history and findings of ophthalmoscopy, but diagnostic imaging is essential for both detailed assessment and monitoring the course of the disease. Fluorescein angiography (FA) has conventionally been the most important method for examining retinal circulation [1], and is still used for a wide range of conditions. Optical coherence tomography (OCT) is a noninvasive method of observing changes in retinal morphology due to impaired retinal circulation [2,3].

In recent years, OCT angiography (OCTA) has enabled noninvasive acquisition of three-dimensional images of retinal perfusion [4]. FA images are two-dimensional, and do not permit separate evaluation of different layers. Tiny structural changes are also difficult to assess. OCTA enables the analysis of any desired layer as well as examination of microvascular structures, and is particularly useful for retinal vascular disorders. A number of recent reports have described OCTA findings in CRAO [5,6].

Several previous studies have addressed the association between CRAO findings and the prognosis in terms of visual acuity. Schmidt *et al.* [7] graded CRAO as incomplete, subtotal, or total on the basis of the severity of visual impairment, the extent of retinal edema, and signs of perfusion on FA, and reported the association between this classification and post-treatment prognosis. Ahn *et al.* [8] investigated spectral-domain OCT (SD-OCT) findings of patients at these three grades, and Furashova *et al.* [9] examined SD-OCT inner layers individually and investigated the intensity of reflectivity.

The objective in this study was to examine swept-source OCT (SS-OCT) images from CRAO patients, and to investigate the associations between their characteristics and prognosis for visual acuity.

Methods

This study protocol was evaluated by the Institutional Review Board and Ethics Committee of Gunma University Graduate School of Medicine, with all investigations conducted in accordance with the Declaration of Helsinki. All subjects provided informed consent for participation in this research.

Study subjects were patients with CRAO examined in the Department of Ophthalmology at Gunma University Hospital who underwent SS-OCTA during the acute phase between May 2017 and December 2018. Patients who were also suffering from other retinal vascular disorders or with previous ocular trauma were excluded. The diagnosis of CRAO was based on findings from ophthalmoscopy (opaque fundus with cherry red spot), SS-OCT (inner retinal hyperreflectivity and thickening), or other imaging modalities. All patients except patient 10 were treated with eye massage at initial examination and 3-day intravenous infusion of alprostadil alfadex 40 µg. No patient was treated with endovascular thrombolytic therapy. All patients underwent SS-OCTA scanning using a PLEX Elite9000® system (Carl Zeiss, Dublin, California, USA) under 6 mm ´ 6 mm scanning conditions within 10 days of onset. The superficial and deep layers of the retina were identified using the preset slab software settings. The border of the superficial layer of the retina was defined as extending from the inner limiting membrane (ILM) to the inner plexiform layer (IPL), and the IPL was defined as 70% of the depth from the ILM to the outer plexiform layer (OPL). The border of the deep layer of the retina was defined as extending from the IPL to the OPL, and the OPL was defined as a 110-µm thick layer superficial to the retinal pigment epithelium. Segmentation errors due to causes such as retinal edema were corrected manually by author and co-authors (H.A., M.M.). Retinal thickness was measured using B-mode images scanned by SS-OCT (DRI OCT-1 Atlantis, Topcon, Tokyo, Japan) at three points: the central fovea, and points 1 mm temporal and 1 mm nasal to the central fovea [10]. The retinal thickness of the unaffected eye was also measured at the same three points as a control. Best-corrected visual acuity was recorded during follow-up. Differences between the two groups were tested for significance using a Mann-Whitney U test, with values of $p < 0.05$ regarded as statistically significant. Statistical analyses were performed using IBM SPSS Statistics version 25 (IBM, Armonk, New York, USA).

Results

Study subjects comprised 11 eyes in 11 patients (8 men, 3 women). Mean age was 73.6 ± 8.8 years (range, 50–86 years), and mean follow-up was 41.9 ± 8.0 days (range, 29–52 days). Mean best-corrected logMAR visual acuity at initial examination was 1.80 ± 0.82. Table 1 shows the characteristics of each patient.

BCVA, best-corrected visual acuity; N/A, not available; CF, count finger; HM, hand motion; HT, hypertension; ASO, Atherosclerosis obliterans; LS, light sense; DM, diabetes mellitus; Fern, fern-like pattern of hyporeflection; Diffuse, diffuse hyperreflection without fern-like pattern; DIV, intravenous Alprostadil Alfadex 40 µg for 3 days; PO, oral administration of Limaprost Alfadex for 1 month; OD, right eye; OS, left eye.

Acute-phase SS-OCT B-mode images revealed hyperreflectivity in the inner retinal layer in all cases. Mean retinal thicknesses of the CRAO-affected eye and unaffected eye were 259 ± 71 μm and 209 ± 25 μm at the central fovea (p = 0.101), 424 ± 86 μm and 305 ± 28 μm on the temporal side (p < 0.001), and 457 ± 121 μm and 318 ± 29 μm on the nasal side (p = 0.002), respectively. This indicated the presence of retinal thickening due to parafoveal retinal edema in the CRAO-affected eye. Acute-phase deep-layer *en face* images revealed overall hyperreflectivity in all cases, compared with the unaffected eye. In some patients, hyporeflective fern-like patterns aligned with arterioles in the arcade were apparent. The four patients (36%) who exhibited these fern-like patterns were grouped together as Group A (Figures 1-3), and the other seven (67%) as Group B (Figures 4,5).

A comparison of best-corrected visual acuity at initial examination in the two groups revealed that logMAR visual acuity was 1.21 ± 1.09 in Group A and 2.15 ± 0.24 in Group B, with a non-significant difference (p = 0.230), visual acuity at 1 month after onset was significantly better in Group A (0.02 ± 0.10) than in Group B (1.51 ± 0.44; p = 0.006) (Figure 6). A comparison of acute-phase retinal thicknesses in Groups A and B found that these were 230 ± 74 μm and 276 ±68 μm at the central fovea (p = 0.164), 371 ± 70 μm and 455 ± 79 μm on the temporal side (p = 0.109), and 381 ± 84 μm and 500 ± 118 μm on the nasal side (p = 0.109), respectively, with no significant differences between groups. Retinal thicknesses in Groups A and B at 1 month after onset were 221 ± 38 μm and 188 ± 25 μm at the central fovea (p = 0.230), 314 ± 36 μm and 251 ± 30 μm on the temporal side (p = 0.042), and 317 ± 35 μm and 260 ± 31 μm on the nasal side (p = 0.024), showing significantly thinning on the temporal and nasal side in Group B. In all patients, hyperreflectivity on deep-layer *en face* images had diminished at 1 month after onset, and now formed a mosaic pattern.

Discussion

Retinal edema and hyperreflectivity of the retinal inner layer are known as characteristic manifestations of OCT B-mode images in acute CRAO [2,3]. All patients in this study also had hyperreflectivity of the retinal inner layer on OCT B-mode images, and overall hyperreflectivity was also evident on deep-layer *en face* images. In four eyes, a hyporeflective fern-like patterns aligned with the arterioles in the arcade. The prognosis for visual acuity for those four eyes was significantly better than for the other seven, and retinal thinning at 1 month after onset also tended to be milder. This finding suggests that hyporeflective fern-like patterns in the acute phase may be a positive prognostic sign.

Bonnin *et al.* [11] investigated the association between the superficial and deep capillary plexuses using OCTA. They suggested a model of supply from the superficial retinal arterioles to the deep capillary plexus directly beneath, forming polygonal lobules, with these converging into vortices that drain into the superficial venules directly above. On the basis of this model, an arterial vascular plexus exists directly beneath the superficial arterioles, and a venous vascular plexus exists directly beneath the superficial venules. If the central artery is only mildly occluded, perfusion in the deep retinal tissue aligned with the superficial retinal arterioles is maintained, and this may appear as a hyporeflective fern-like pattern in *en face* images.

The area defined as the deep layer of the retina on OCTA is centered on the inner nuclear layer (INL). In studies measuring intraretinal oxygen partial pressure in cats and rats [12,13], values were lower in the middle layer of the retina corresponding to the INL than in either the inner or outer layers of the retina. OCTA images of the deep layer of the retina can thus easily reflect the effect of ischemia in the retinal arteries, enabling diffuse hyperreflectivity and fern-like patterns to be more clearly observed on *en face* images.

Paracentral acute middle maculopathy (PAMM) is a recently proposed disease concept characterized by hyperreflectivity of the middle layer of the retina on OCT [14]. PAMM is often present in association with other retinal vascular disorders, and is believed to reflect capillary ischemia of the deep layer of the retina. Sridhar *et al.* [15] categorized *en face* images from PAMM patients into three patterns, one of which they reported as a fern-like pattern similar to that observed in this study. Sridhar *et al.* considered that the mechanism underlying this fern-like pattern was paravenular ischemia of the vascular plexus in the retina. Garrity *et al.* [16] suggested that the mechanism underlying the fern-like pattern seen in central retinal vein occlusion was secondary arterial hypoperfusion due to elevated venous pressure caused by venous occlusion. Falavarjani *et al.* [17] examined 11 eyes with PAMM that exhibited fern-like patterns, and found that although 7 represented typical cases of retinal vein occlusion, no specific fundus signs were visible in the other 4. They suggested that those 4 cases may have represented primary arterial hypoperfusion, despite the absence of any clear signs of arterial occlusion. None of our CRAO patients also suffered from venous occlusion, and the fern-like pattern we observed in this study was highly likely to be due to primary arterial hypoperfusion caused by CRAO.

This study had a number of limitations. As this was a retrospective study of a comparatively small number of patients in single-center, further investigations of larger cohorts are required in the future. The mechanism underlying the fern-like pattern can only be conjectured on the basis of OCT and OCTA findings and other reported studies.

Conclusions

The fern-like pattern we observed in *en face* images in this study may indicate a good prognosis for visual acuity, a finding that may be helpful in the future management of CRAO.

Abbreviations

CRAO : Central retinal artery occlusion

FA : Fluorescein angiography

OCT : Optical coherence tomography

OCTA : OCT angiography

SD-OCT : Spectral-domain OCT

SS-OCT : Swept-source OCT

ILM : Inner limiting membrane

IPL : Inner plexiform layer

OPL : Outer plexiform layer

INL : Inner nuclear layer

PAMM : Paracentral acute middle maculopathy

Declarations

Ethics approval and consent to participate

This study protocol was evaluated by the Institutional Review Board and Ethics Committee of Gunma University Graduate School of Medicine, with all investigations conducted in accordance with the Declaration of Helsinki. All subjects provided informed consent for participation in this research.

Consent for publication

Not applicable

Availability of data and material

The datasets used and/or analyzed during the current study are available from the corresponding author on reasonable request.

Competing interests

The authors declare that they have no competing interests

Funding

Not applicable

Authors' contributions

JH acquired and analyzed data and was a major contributor in writing the manuscript. HA designed this work and analyzed data. MM acquired and analyzed data. RM and HM revised this work. All authors read and approved the final manuscript.

Acknowledgements

Not applicable

References

1. David NJ, Norton EWD, Gass JD, Beauchamp J. Fluorescein Angiography in Central Retinal Artery Occlusion. Arch Ophthalmol 1967;77: 619-29.
2. Wada M. Optical coherence tomographic features of retinal artery occlusions. Jpn J Clin Ophthalmol 1998;52:1531-4.
3. Suto K, Hagimura N, Iida T, Kishi S. Retinal tomographic images in central retinal artery occlusion. Jpn J Clin Ophthalmol 2001;55:905-8.
4. Spaide RF, Klancnik JM Jr, Cooney MJ. Retinal Vascular Layers Imaged by Fluorescein Angiography and Optical Coherence Tomography Angiography. JAMA Ophthalmol 2015;133:45-
5. Philippakis E, Dupas B, Bonnin P, Hage R, Gaudric A and Tadayoni R. Optical coherence tomography angiography shows deep capillary plexus hypoperfusion in incomplete central retinal artery occlusion. Retinal Cases and Brief Reports 2015;9:333-8.
6. Damento G, Chen MH, Leng T. Spectral-domain optical coherence tomography angiography of central retinal artery occlusion. Ophthalmic Surgery, Lasers and Imaging Retina 2016;47:467-
7. Schmidt D, Schumacher M. Stage-dependent efficacy of intra-arterial fibrinolysis in central retinal artery occlusion (CRAO). Neuro-ophthalmology 1998;20:125-41.
8. Ahn SJ, Woo SJ, Park KH, Jung C, Hong JH, Han MK. Retinal and choroidal changes and visual outcome in central retinal artery occlusion: an optical coherence tomography study. Am J Ophthalmol 2015;159:667-76.
9. Furashova O, Matth´e E. Retinal Changes in Different Grades of Retinal Artery Occlusion: An Optical Coherence Tomography Study. IOVS 2017;58:5209-16.
10. Ikeda F, Kishi S. Inner Neural Retina Loss in Central Retinal Artery Occlusion. Jpn J Ophthalmol 2010;54:423-9.
11. Bonnin S, Mané V, Couturier A, Julien M, Paques M, Tadayoni R, et al. New insight into the macular deep vascular plexus imaged by optical coherence tomography angiography. RETINA 2015; 35: 2347-52.
12. Lisenmeier RA. Effects of light and darkness on oxygen distribution and consumption in the cat retina. J Gen Physiol 1986; 88:521-42.
13. Yu DY, Cringle SJ, Alder V, Su EN. Intraretinal oxygen distribution in the rat with graded systemic hyperoxia and hypercapnia. Invest Ophthalmol Vis Sci 1999;40:2082-7.
14. Sarraf D, Rahimy E, Fawzi AA, Sohn E, Barbazetto I, Zacks DN, et al. Paracentral Acute Middle Maculopathy A New Variant of Acute Macular Neuroretinopathy Associated With Retinal Capillary Ischemia. JAMA Ophthalmol 2013;131:1275-87.

15. Sridhar J, Shahlaee A, Rahimy E, Hong BK, Khan MA, Maguire JI, et al. Optical Coherence Tomography Angiography and En Face Optical Coherence Tomography Features of Paracentral Acute Middle Maculopathy. Am J Ophthalmol 2015;160:1259-68.
16. Garrity ST, Tseng VL, Sarraf D. Paracentral acute middle maculopathy in a perivenular fern-like distribution with en face optical coherence tomography. Retin Cases Brief Rep. 2018;12:25-8.
17. Falavarjani KG, Phasukkijwatana N, Freund KB, Cunningham ET, Kalevar A, Macdonald HR, et al. En face OCT analysis to assess the spectrum of perivenular ischemia and paracentral acute middle maculopathy in retinal vein occlusion. Am J Ophthalmol 2017;177:131-8.

Tables

Table 1. Summary Data of Patients.

Patient	Age	Sex	Eye	Systemic diseases	Duration to OCTA	OCT en face pattern	Presenting BCVA	Final BCVA	PGE1 treatment	Follow-up
1	76	M	OS	N/A	10 days	Fern	20/400	20/25	DIV+PO	45 days
2	75	F	OD	HT	1 days	Diffuse	HM	20/500	DIV	52 days
3	50	M	OS	N/A	10 days	Fern	LS -	20/16	DIV	39 days
4	81	F	OD	N/A	12 hours	Diffuse	CF	20/200	DIV	43 days
5	70	M	OD	HT	1 day	Diffuse	20/1000	20/320	DIV+PO	50 days
6	86	M	OS	HT,DM	1 day	Fern	20/16	20/16	DIV	29 days
7	75	M	OD	N/A	1 day	Diffuse	HM	20/200	DIV+PO	36 days
8	76	M	OS	HT	10 days	Diffuse	HM	20/630	DIV+PO	51 days
9	72	M	OD	HT	1 days	Diffuse	HM	HM	DIV+PO	31 days
10	80	F	OD	ASO	2 days	Fern	20/100	20/32	N/A	50 days
11	69	M	OD	N/A	1 days	Diffuse	HM	20/333	DIV	35 days

Figures

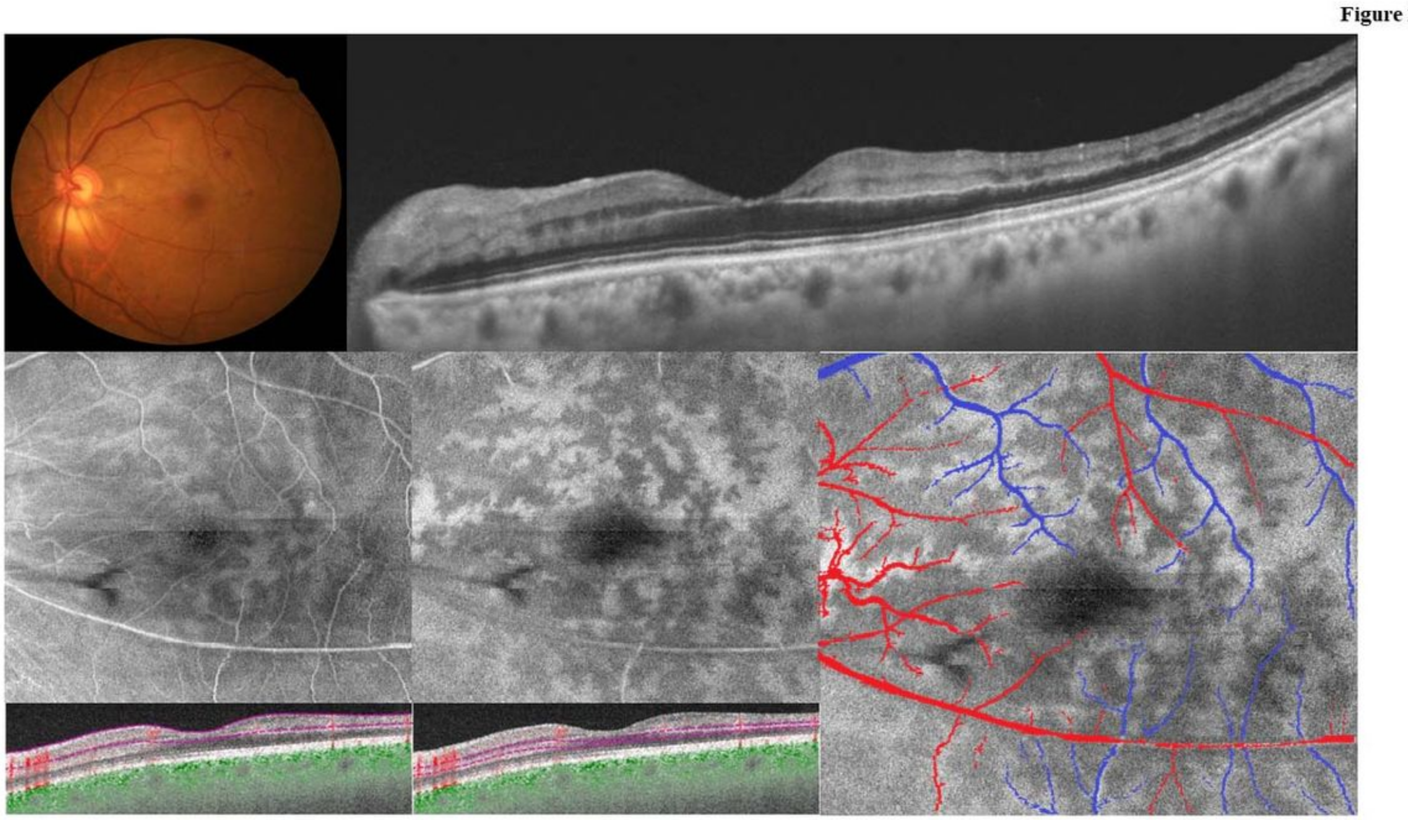

Figure 1

Acute phase in Patient 1 (Group A). White opacity is visible in the posterior pole of the fundus (top left). On OCT B-mode image, hyperreflectivity is evident from the middle layer to the inner layer of the retina (top right). Hyperreflectivity distributes like a mosaic in the superficial layer (center left), but a fern-like pattern is clearly visible in the deep layer (center middle). In a deep-layer en face image with superficial arterioles indicated in red and superficial layer venules in blue (bottom right), hyporeflective areas are aligned with the courses of the arterioles.

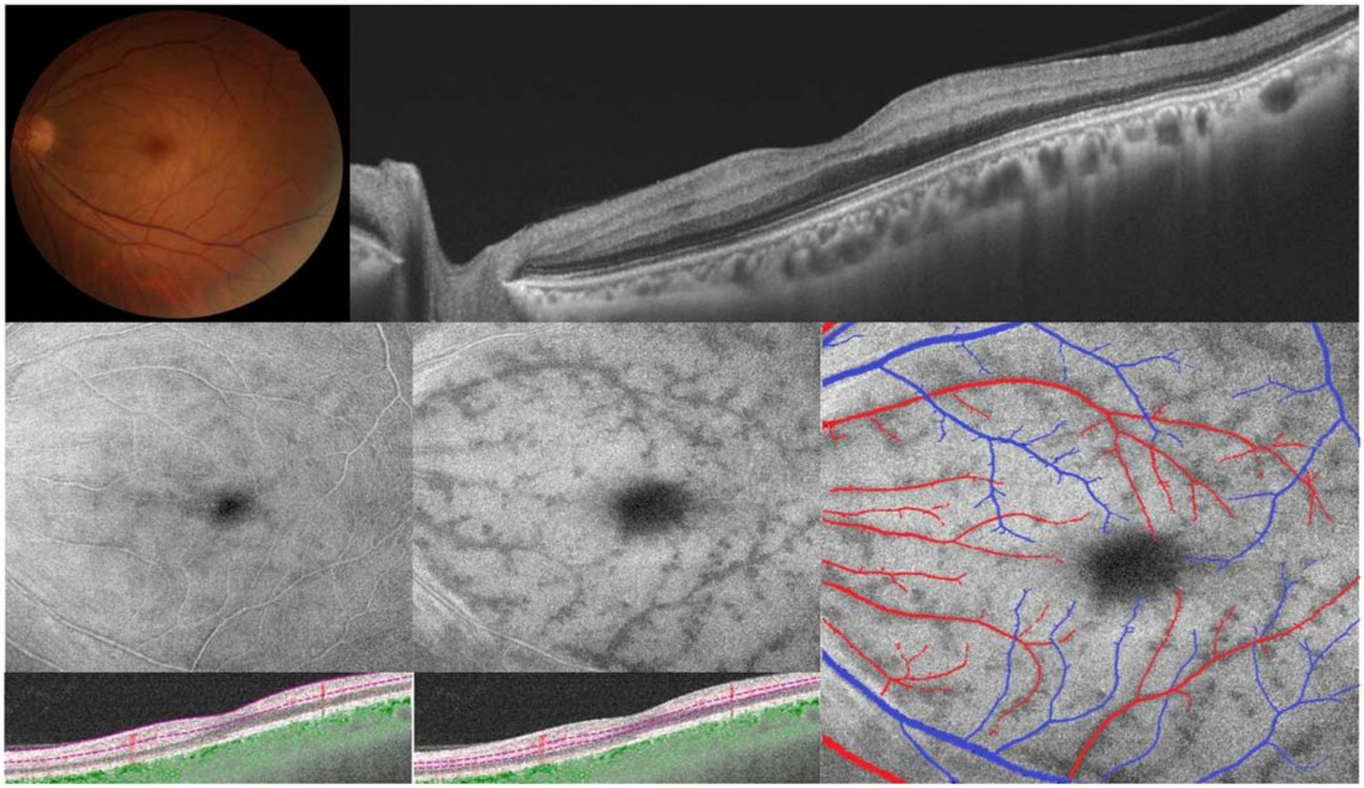

Figure 2

Acute phase in Patient 3 (Group A). Retinal whitening is seen in the posterior pole (top left). On OCT B-mode image, hyperreflectivity is visible from the middle layer to the inner layer of the retina (top right). En face image reveals hyperreflectivity in the superficial layer (center left) and a fern-like pattern in the deep layer (center middle). Hyporeflective areas are aligned with the courses of the arterioles (bottom right).

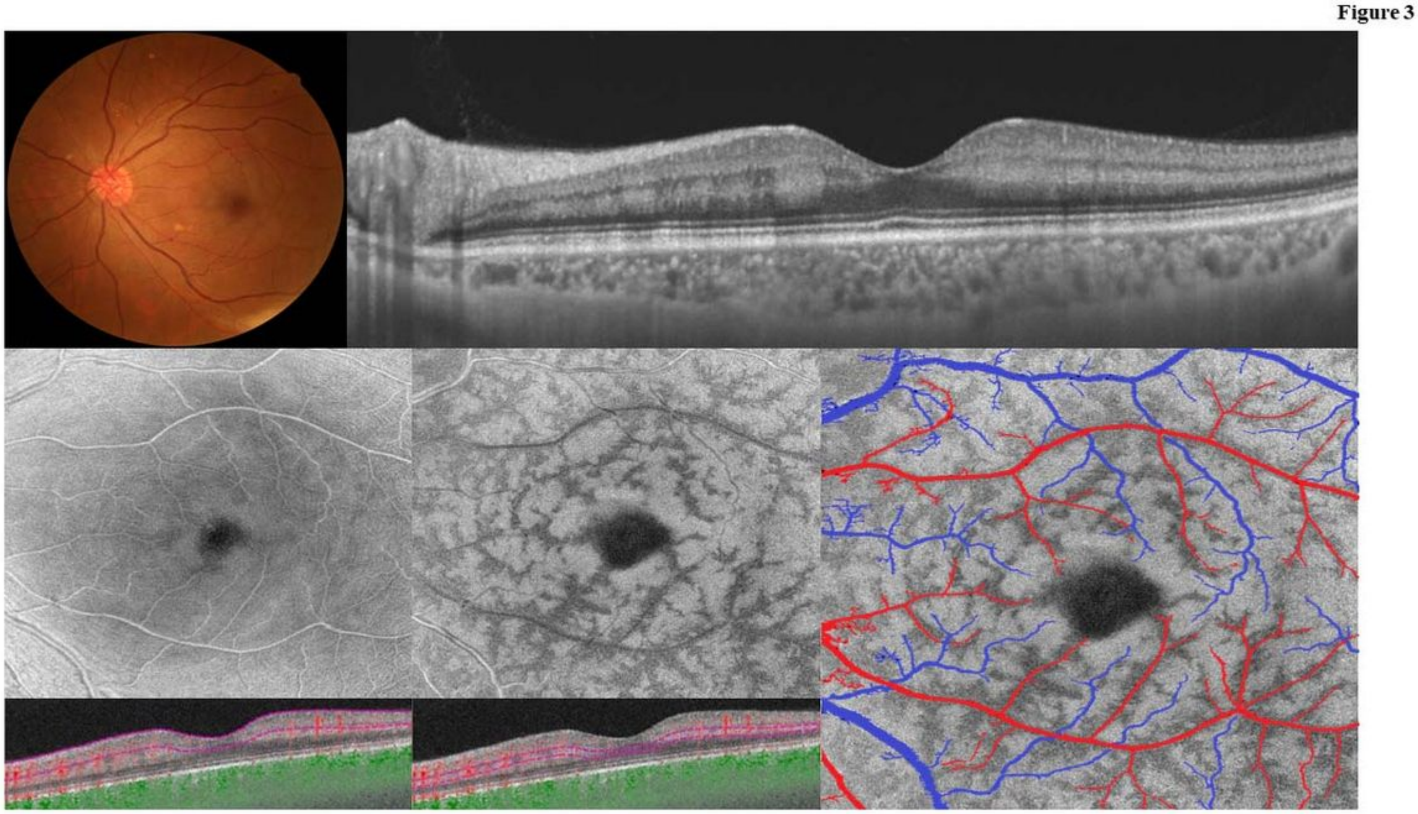

Figure 3

Acute phase in Patient 6 (Group A). Mild macular whitening is visible in the posterior pole (top left). OCT B-mode image reveals hyperreflectivity from the middle layer to the inner layer of the retina (top right). Hyperreflectivity is mild in the superficial layer (center left), but a fern-like pattern is clearly visible in the deep layer (center middle). Similar to the other cases showing a fern-like pattern, hyporeflective areas are aligned with the courses of the arterioles (bottom right).

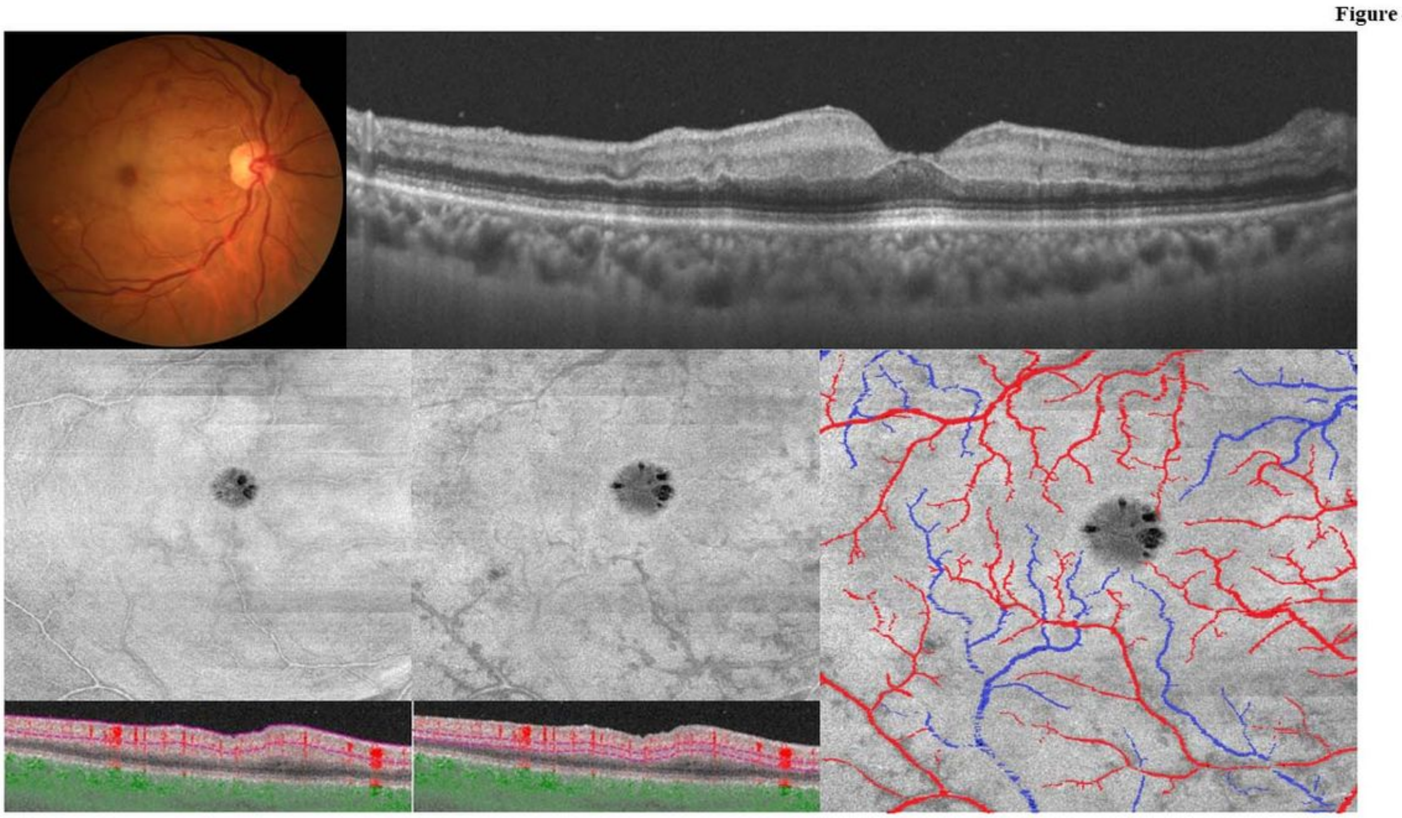

Figure 4

Acute phase in Patient 6 (Group A). Mild macular whitening is visible in the posterior pole (top left). OCT B-mode image reveals hyperreflectivity from the middle layer to the inner layer of the retina (top right). Hyperreflectivity is mild in the superficial layer (center left), but a fern-like pattern is clearly visible in the deep layer (center middle). Similar to the other cases showing a fern-like pattern, hyporeflective areas are aligned with the courses of the arterioles (bottom right).

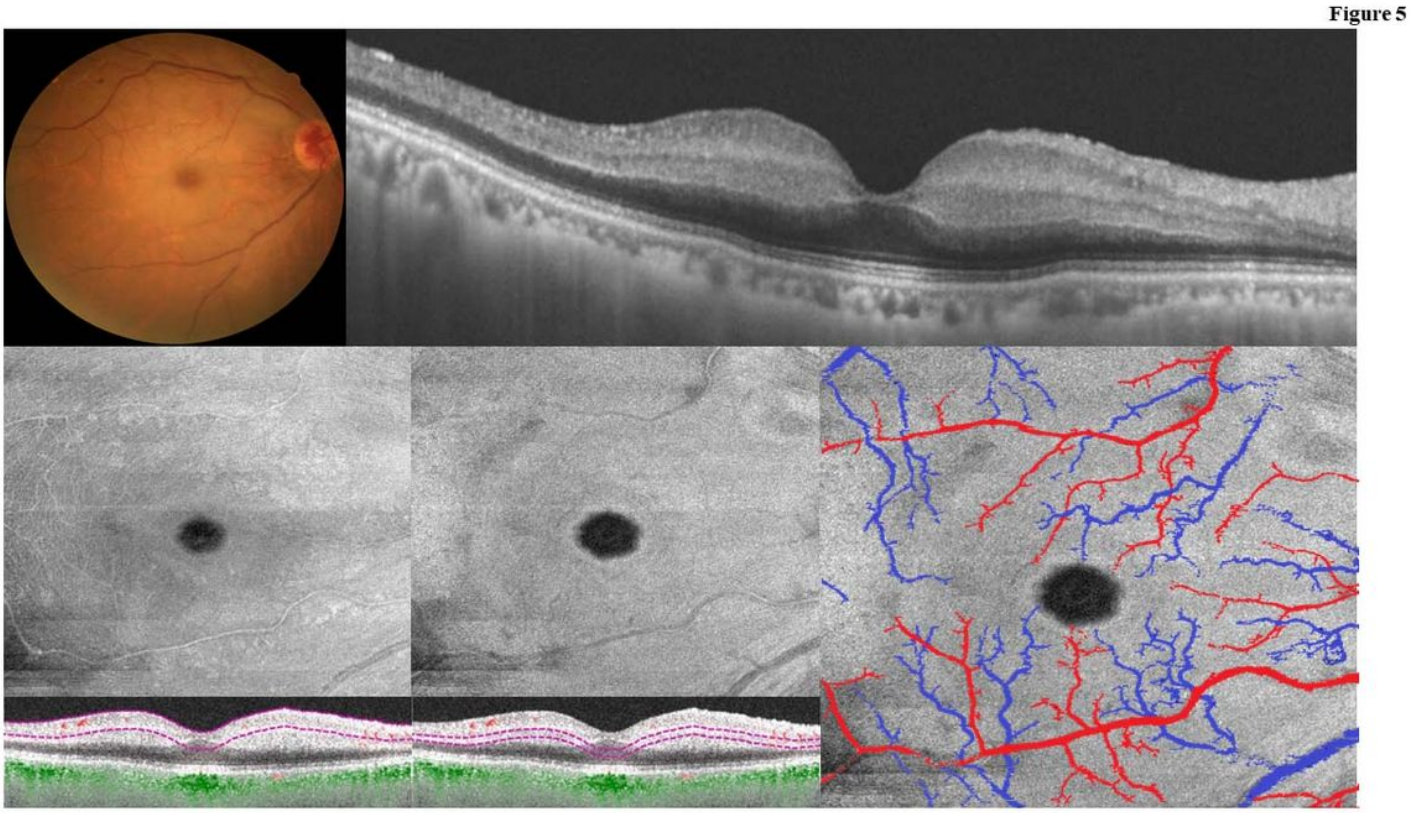

Figure 5

Acute phase in Patient 2 (Group B). Retinal whitening and cherry red spot are visible in the posterior pole (top left). OCT B-mode image reveals retinal edema and hyperreflectivity in the inner layer and the middle layer of retina (to right). Diffuse hyperreflectivity is apparent in both the superficial layer (center left) and deep layer (center middle), with no correspondence with the courses of superficial vessels (bottom right).

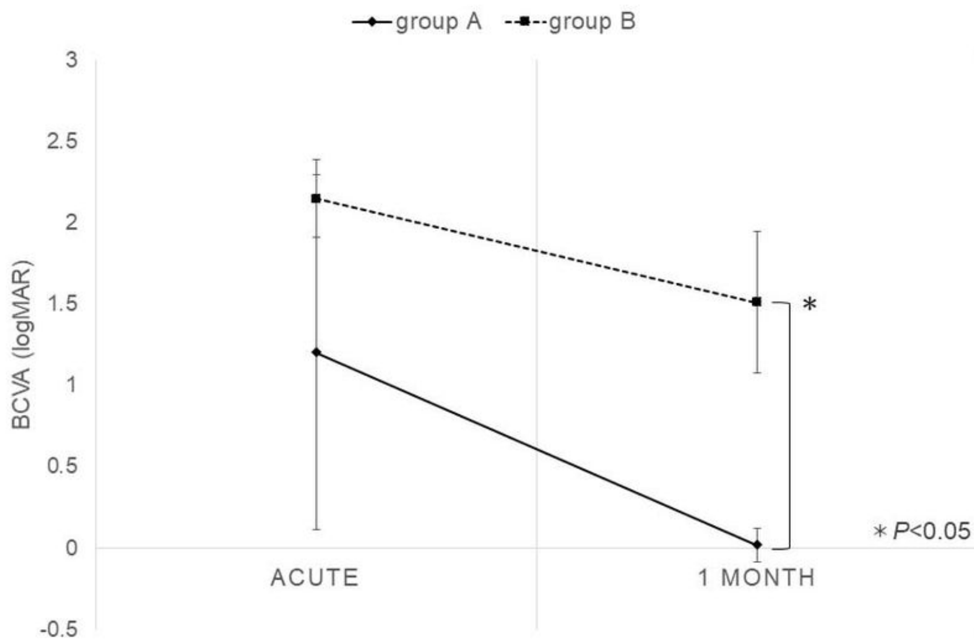

Figure 6

Changes in best corrected visual acuity (logMAR). Visual acuity at 1 month after onset was significantly better in Group A (0.02±0.10) than in Group B (1.51±0.44; p=0.006)